Journal of Applied Polymer Science

Investigating the Self Healing Process on Coated Steel by SVET and EIS Techniques

S. Neema,[1] M. Selvaraj,[2] J. Raguraman,[2] S. Ramu[2]

[1]Department of Chemistry, University of Calicut, Calicut

[2]CSIR-Central Electrochemical Research Institute, Karaikudi 630 006, Tamil Nadu, India

Correspondence to: M. Selvaraj (E-mail: selvaraj58@gmail.com)

ABSTRACT: Microencapsule was incorporated into an interpenetrating polymer network and applied over steel surface. A scratch was made on the coated surface and its self healing ability was studied using scanning vibrating electrode technique (SVET) and electrochemical impedance spectroscopy (EIS). Results of SVET studies show that the current density increases in the initial stage. After 24 h, the current density decreases, which indicating the formation of passive polymer film due to the diffusion of core polymer present in the microcapsules through the holidays. Increase in the resistance (10^7 Ω/cm^2) of the self healing coating was observed after 24 h in EIS studies confirming the formation of the passive film. The results of the studies are discussed in this article. © 2012 Wiley Periodicals, Inc. J. Appl. Polym. Sci. 000: 000–000, 2012

KEYWORDS: interpenetrating polymer network; microencapsule; self healing effect; scanning vibrating electrode techniques; electrochemical impedance spectroscopy

Received 25 August 2011; accepted 18 March 2012; published online
DOI: 10.1002/app.37791

INTRODUCTION

Corrosion protective coatings should provide not only a barrier to the environment, but also act by the smart release of polymer materials in the event of damage to the coating. Smart coating system with self healing properties has been reported by Kumar[1] and White.[2] The coating contains microencapsules, whose core material can be released when damage occurs on the surface. The microcapsules are used to deliver healing agents to terminate the corrosion process in the damaged area at its early stage. This field of release of healing materials to damage area is a relatively new one. Dong Yang Wu et al.[3] explained the method of preparation of the self healing coatings and evaluation of their self healing efficiency. Ding Shu Xiao et al.[4] formulated a self healing coating consists of epoxy capsules incorporated in a coating system containing a cationic catalyst. When a cracks occur in the composite coating, the healing system quickly rebond with satisfactory healing efficiency.

Interpenetrating polymer network (IPN) technology is of importance for a wide range of applications especially in coatings. Silicone based 1PNs have received much attention in the field of protective coatings for high temperature application.[5–7] In recent years, conducting polymer has been used as inhibitors for corrosion protection. The protective mechanism of conducting polymers is ascribed to the intelligent release of inhibitor anions. However, conducting polymers fail to protect large defective areas, although they offer excellent protection to small defects.[8] Studies of Ocampo et al.[9] indicate that the conducting polymer incorporated coatings give a 10-fold protection when compared to coatings without this conducting polymer; they are also stable for high temperature applications. The thermal stability of conducting polymer based IPNs has improved considerably. Conducting polymer based IPNs are widely used in activators,[10] but their use in protective coating is limited. Acrylic polymers have excellent chemical resistance and glassy appearance and so it interpenetrated with Silicone polymer to generate new high performance polymer.

In this study an IPN was prepared by silicone resin, acrylic monomers, and additives. The 1PN was characterized by FTIR, TGA/DSC, and GPC. Microencapsules were prepared by interfacial polymerization process. These microencapsules were incorporated in the IPN and coated on steel substrate. Performance of the self healing coating in 0.05*M* sodium chloride solution was investigated using scanning vibrating electrode technique (SVET) and electrochemical impedance spectroscopy (EIS).

EXPERIMENTAL

Preparation of Microencapsules by Interfacial Polymerization

Materials. Urea, formaldehyde ammonium chloride, hydrochloric acid, resorcinol ethylene maleic anhydride, and triehanolamine were obtained from Qualingens Fine Chemicals. Butyl-2,3-epoxy propyl ether (E-Merck) and Epoxy resin (Ciba-Geigy) were used as received.

In a three necked flask, 5 g of urea was dissolved in 100 mL double distilled water at room temperature; 0.5 g of ammonium chloride and 0.5 g of resorcinol were added to it. Ethylene maleic anhydride solution (2%) was added and pH was adjusted to 8–9 using triethanolamine. Temperature of the system was kept at 333 K for 1 h. Then 60 g of liquid epoxy polymer (epoxy equivalent 225–250) and 5 g of butyl-2,3-epoxy propyl ether was added. The solution was agitated at 500 rpm and 10 g of 37 wt % formaldehyde solution was added for the formation of urea formaldehyde shell material. These shell resins encapsulate the epoxy resin as core substance for the formation of microencapsules. After stirring for 30 min, the pH of the solution was adjusted slowly to 3–4 using 10 wt % of hydrochloric acid to harden the shell substrate and the solution was heated to 333 K. After 1 h, the suspended microencapsules were rinsed with distilled water and filtered and dried for 24 h.

Characterization of Microencapsules

The size distribution of microcapsules and self healing efficiency of the coating were investigated using optical microscope under 100 magnification using Olympus B x 51 M optical microscope and the average size of the capsules was measured on data sets of 100 measurements. The compressive strength of the microcapsules was measured by destruction tester model No.1307R supplied by ALKOH (Japan).

Preparation of IPN

Materials. Methyl methacrylate (E-Merk), Butyl acrylate (E-Merk), Hydroxy ethyl methacrylate (E merk), Silicone polymer (Metro ark), Benzyl peroxide (Qualigens), Dibutyl tin dilaurate (Aldrich), and Xylene (Qualigens) were used as received.

The synthetic method for IPNs had been explained by many researchers.[11,12] We followed the modified version of Meet Kamal's procedure.[13] A series of IPNs were prepared by *in situ* polymerization during which the concentration of the silicone polymer in xylene with acrylic monomers was systematically varied for 15 h at 413 ± 5 K.[14] The unreacted monomer present in the IPN was removed by soxhlet extraction method. The IPN formed was collected in a dried flask and make a 60% volume solid IPN was made using xylene as solvent. The IPN with a molar ratio of Silicone: MMA: BA of 0.005: 0.0559: 0.0546 exhibited excellent heat resistance properties and it was used for the formulation of self-healing coatings.

Characterization of IPN

The functional groups present in the IPN was identified by Fourier Transform Infrared (FTIR) spectroscopy, recorded in the range of 400–4000 cm^{-1} using NE x US 670 (FTIR). Thermal stability of this IPN was ascertained by TGA analysis using universal V4 3A SDT 2600, under a pure nitrogen flow rate of 25 mL/min. The sample and the references were heated at a rate of 20°C/min. The phase changes and the glass transmission temperature of the resin were measured using Perkin–Elmer Differential Scanning Colorimeter, DSC–2.

The average molecular weight and polydispersability of the IPN was determined by software controlled Gel permeation Chromatography (GPC) of Shimaduz CTO-20, RID-10A detector (Japan). In GPC, polystyrene was used as standard and the measurements were made at ambient conditions with Tetra hydro furan as carrier solvent in a carbowax column.

Preparation of Self Healing Composite Coated Panels

Melamine-based hardener was used as catalyst for this composite coating which was dispersed in the IPN. This catalyst incorporated IPN was applied on to pickled mild steel panels of size 7.5 cm × 5 cm by brush. These panels were cured for 15 days and the thickness of the coating was measured using mikrotester and found to be 50 ± 5 μm. Catalyst mixed IPN containing 10% microencapsules was coated on to another set of pickled mild steel panels by brush. These panels were cured for 15 days and the thickness of the coating was measured and found to be 175 ± 5 μm. Coated panels with a scratch of 1 mm width were used for SVET and EIS measurements.

EVALUATION TECHNIQUES

Scanning Vibrating Electrode Technique. Scanning Vibrating Electrode Technique (SVET) measurements were made by Uniscan Instruments (Model: Scanning Electrochemical workstation 370 PAR). A standard SVPCR 973 platinized platinum probe was employed and 0.05*M* sodium chloride solution was used as electrolyte.

This technique gives information about the corrosion initiation in small area. SVET operates by a non-intrusive scanning, vibrating probe measurement, and maps the electric field generated in a plane above the electrochemically active surface. This enables the user to map and quantify local electrochemical and corrosion events in real time. This technique is also useful to study the action of inhibitor coatings for corrosion protection.[15–17]

The SVP370 vibrating probe system provides increased electrical sensitivity as well as enhanced system stability. Localized corrosion events of <5 $\mu A/cm^2$ can be measured by this extremely sensitive technique. The probe vibration is controlled by a piezoceramic displacement device. It is an AC technique, thus, high system sensitivity is achieved through a differential electrometer in conjunction with an integrated lock-in amplifier. All system parameters, including the x–y–z scanning mechanism, piezo lock-in amplifier are controlled by a PC under the user friendly Windows™ operating system.

The prepared specimen was mounted on the specimen holder of SVET apparatus. SVET records only the potential difference across the probe, which is a measure of the local current emanating from the surface. The potential difference was measured by a micro-tip probe made of platinized platinum coated with polymeric material, vibrating in a plane perpendicular to the sample surface at an amplitude of 30 μm. The probe was lowered to the height of 50 μm above the specimen and then the

electrolyte was added to the environmental cell. The area scans were obtained at the scan rate of 100 μm/s and a time constant of 1 s, to collect 82, 26 sample points at X and Y displacements. The time duration of a single scan was 25 min and the experiment was continued for 24 h. All the measurements were taken at open circuit potential. Experiments were repeated for reproducibility.

Electrochemical Impedance Spectroscopy. Use of EIS for the study of corrosion protection by polymer coatings is explained by Mansfeld[18] and suggested the need of qualitatively using modified break point frequency method. Impedance measurement was made at open circuit potential using PAR STAT model 2273, A–C impedance system and a three electrode configuration.

The electrochemical tests were carried out in a quiescent aerated 0.05*M* NaCl solution. The surface area of coated panels exposed to the electrolyte was 1 cm^2. It will serve as working electrode. A three electrode electrochemical cell was formed by sticking a glass tube on the panels and filling it with the solution of the corrosive electrolyte (0.05*M* NaCl solutions). A high surface area platinum mesh and saturated calomel electrode were used as counter and reference electrodes, respectively.

RESULTS AND DISCUSSION

The core polymer present in the microencapsules is given in Table I. It is seen from the table that the size of microcapsules decreases with the increase in the stirring speed. Further, the content of the core polymer decreases with the decreasing size of the capsules, in the mean time the shell material weight is increased. This result indicates that when the stirring speed is at 500 rpm, the core content is of the order of 83.781%. Experimental result of Suriyanarayana et al.[19] indicated that the 80% Linseed oil as a core material in the capsule cured the cracks in a short span of time. So, the urea formaldehyde encapsulated epoxy resin contains 83.781% as core resin is enough to cure the cracks quickly as compared with Suriyanarayana's study. Thus, this type of capsule is enough for self healing coating formulation to heal the damage area in lesser duration.

Size of the microencapsules, as determined by the microscopy method was 125 $\pm$ 5 μm. Samadzadeh et al.[20] indicated that the probable size of the capsule is 125–100 μm at an agitation speed of 500 rpm. The image of microencapsules is shown in the Figure 1. As seen in the figure, the shape of the capsules is spherical in shape and is wide apart. The compressive strength of the capsules is also in low range of 357 g/F. So, the capsules can be easily broken down when a force act on its surface.

Table I. Percentage of Core Polymer and Shell Material Present in the Microcapsules in Different Stirring Speed

Stirring speed (r.p.m)	Core polymer (%)	Shell material (%)
500	83.781	16.219
700	82.727	17.273
1000	80.635	19.345

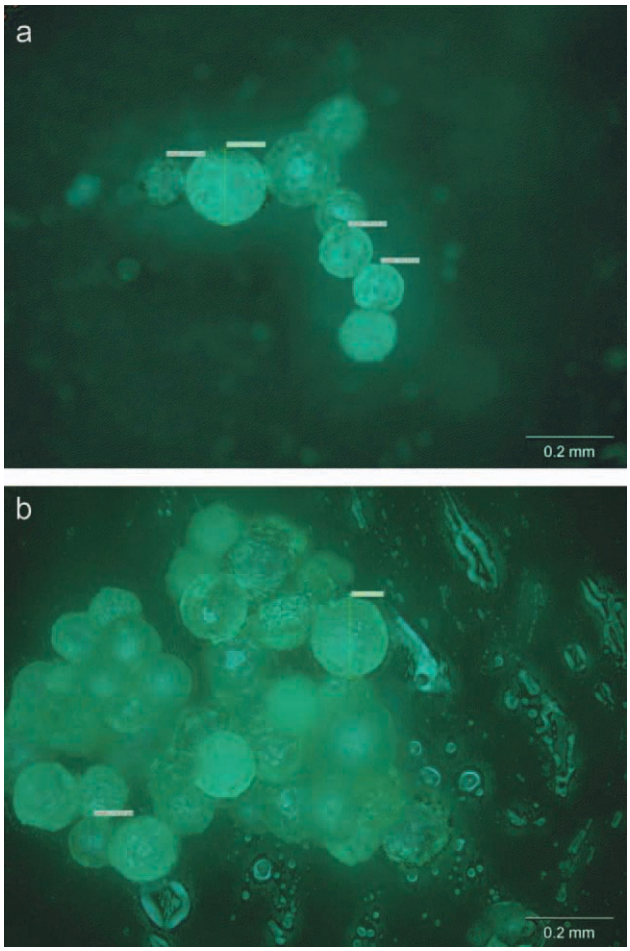

Figure 1. Optical microscopic images of microcapsules. [Color figure can be viewed in the online issue, which is available at wileyonlinelibrary.com.]

Characterization of IPN

Molecular weight of the silicone resin is 14,708 and that of the IPN is 11,276. The ratio of weight average molecular weight and the number average molecular weight of the IPN is 1.0856.

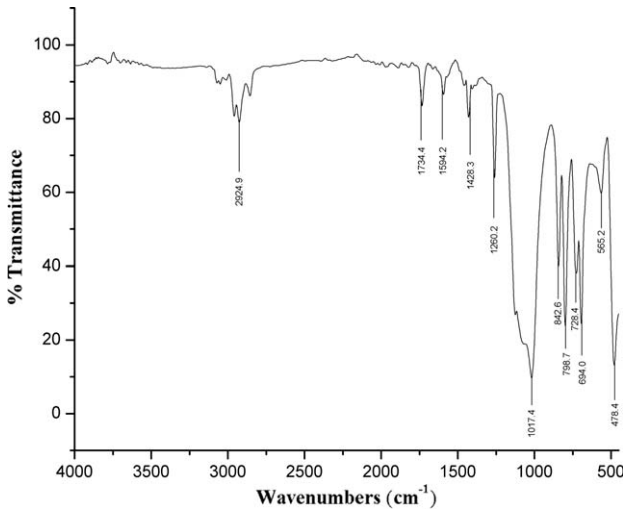

Figure 2. FTIR spectrum of inter penetrating polymer network (IPN).

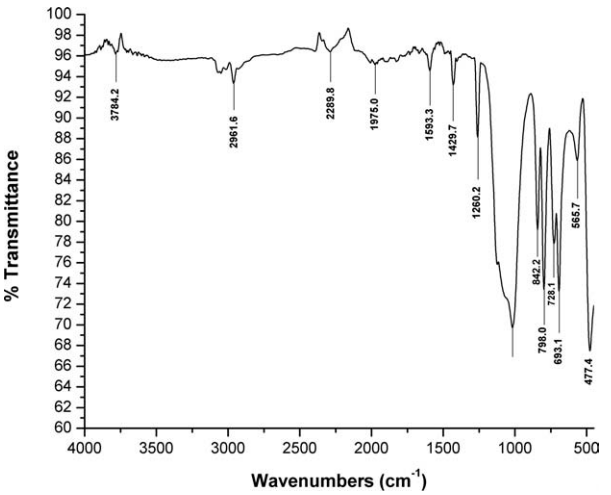

Figure 3. FTIR spectrum of silicone polymer.

This indicates that the formation of the IPN is in homogeneous state.

(a) FTIR. The FTIR spectrum of silicone acrylic IPN is shown in Figure 2. The broad doublet peaks observed at 2924.9 cm^{-1} is the indication of methyl and methylene group vibration of the acrylic linkages in the polymer. Similarly, the doublet peaks at 1428.3 cm^{-1} corresponds to the $–CH_2–$ deformation vibration. The carbonyl group present in the IPN is indicated by the appearance of sharp peak at 1734.3 cm^{-1}.[21,22] The characteristic silicone linkages of –Si–O–Si–, $–Si–CH_3$ are indicated by the sharp peaks at 1260.2 cm^{-1} and 478.4 cm^{-1}. It can be seen that the major groups, namely, $–CH_3$ and –OH are directly attached to the silicone resin. The broad peaks at 1138 cm^{-1} is due to Si–O linkage and the broad bond at 1017.4 cm^{-1} is due to the presence of Si–O–C linkage in the silicone IPN polymer.[23,24] The characteristic carbonyl group peak at 1734.3 cm^{-1} is completely absent in silicone resin (Figure 3). Further, the broad band for the Si–H linkage is also absent in the IPN. The broad peak and band for Si–O–C linkages are present in the IPN. Thus, the formation of IPN from silicone and acrylic monomers is confirmed.

Thermal Stability

Figure 4 shows the TGA and DSC curves of silicone resin used for the formation of IPN. The TGA for the silicone resin shows an almost horizontal line upto 562.62 K with a weight loss of 2.01%. This indicates that silicone polymer is stable even at high temperature. This small weight loss is due to the evaporation of superficial solvent molecules present in the resin. Degradation starts from this temperature and reach a steady state at 873 K with a weight loss of 44.36%. This indicates that the Si–C linkages in the polymers are broken and small molecules like CO_2, H_2O are liberated from the polymer. The higher weight retention of the polymer is due to the formation of stable silica.

Similar behavior is also observed in the DSC studies. It is observed from the figure that no thermal reaction takes place with the liberation or absorption of energy. A small exothermic reaction occurs at about 723.24 K. This indicates that the silicone based polymer is thermally stable at high temperature.

TGA/DSC profile of silicone–Acrylic IPN is given in Figure 5. The thermogram shows that the degradation temperature is lower than that of silicone resin. IPN starts to decompose at 484.23 K with a weight loss of 1.91%. This weight loss is mainly due to the evaporation of the acrylic monomers present in the IPN. After 484.23 K, the IPN decomposes with a weight loss of

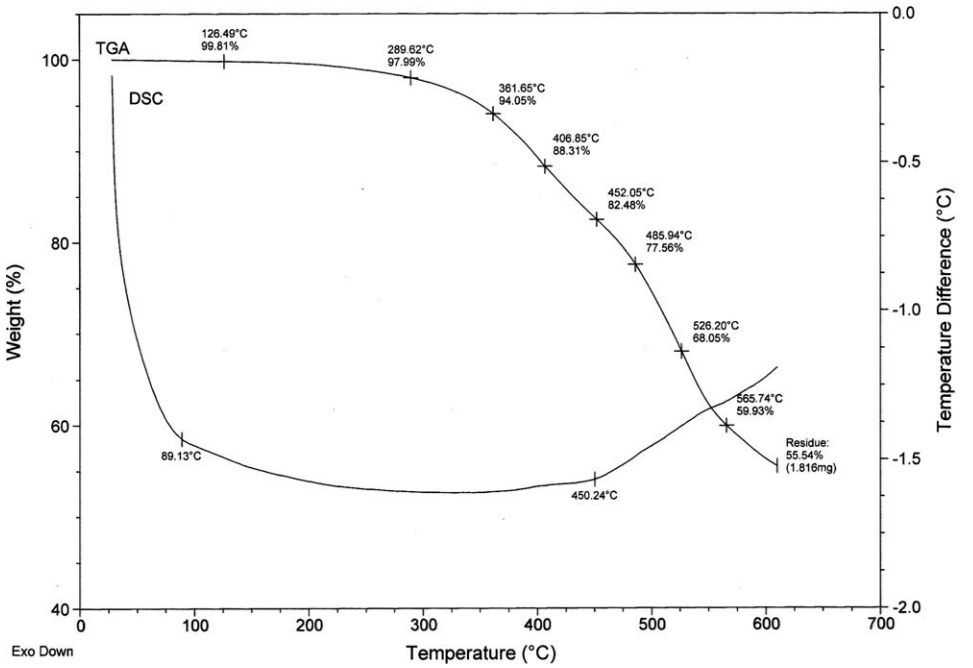

Figure 4. TG/DSC diagram of silicone resin.

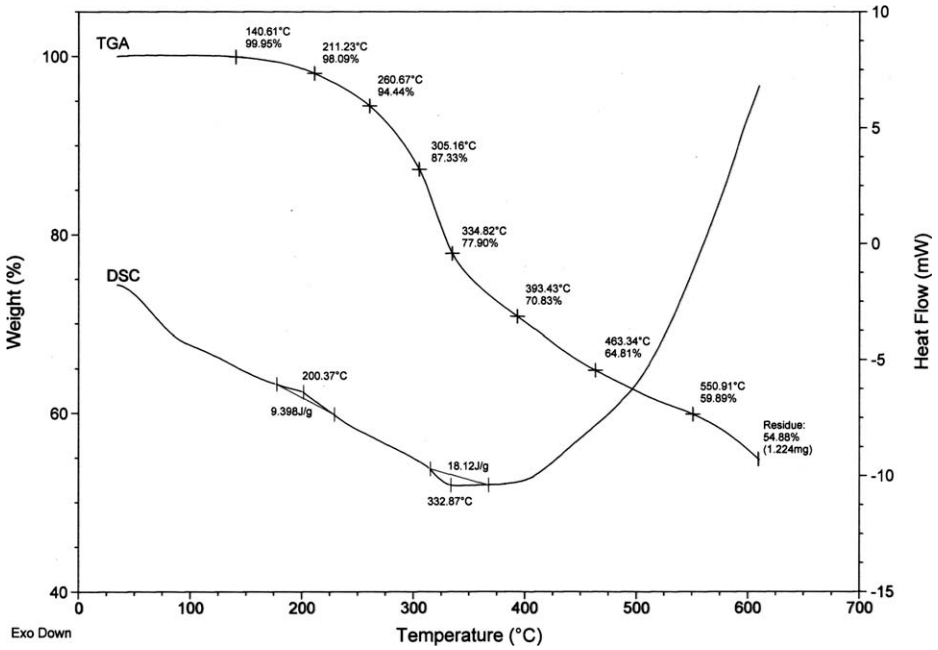

Figure 5. TG/DSC diagram of IPN.

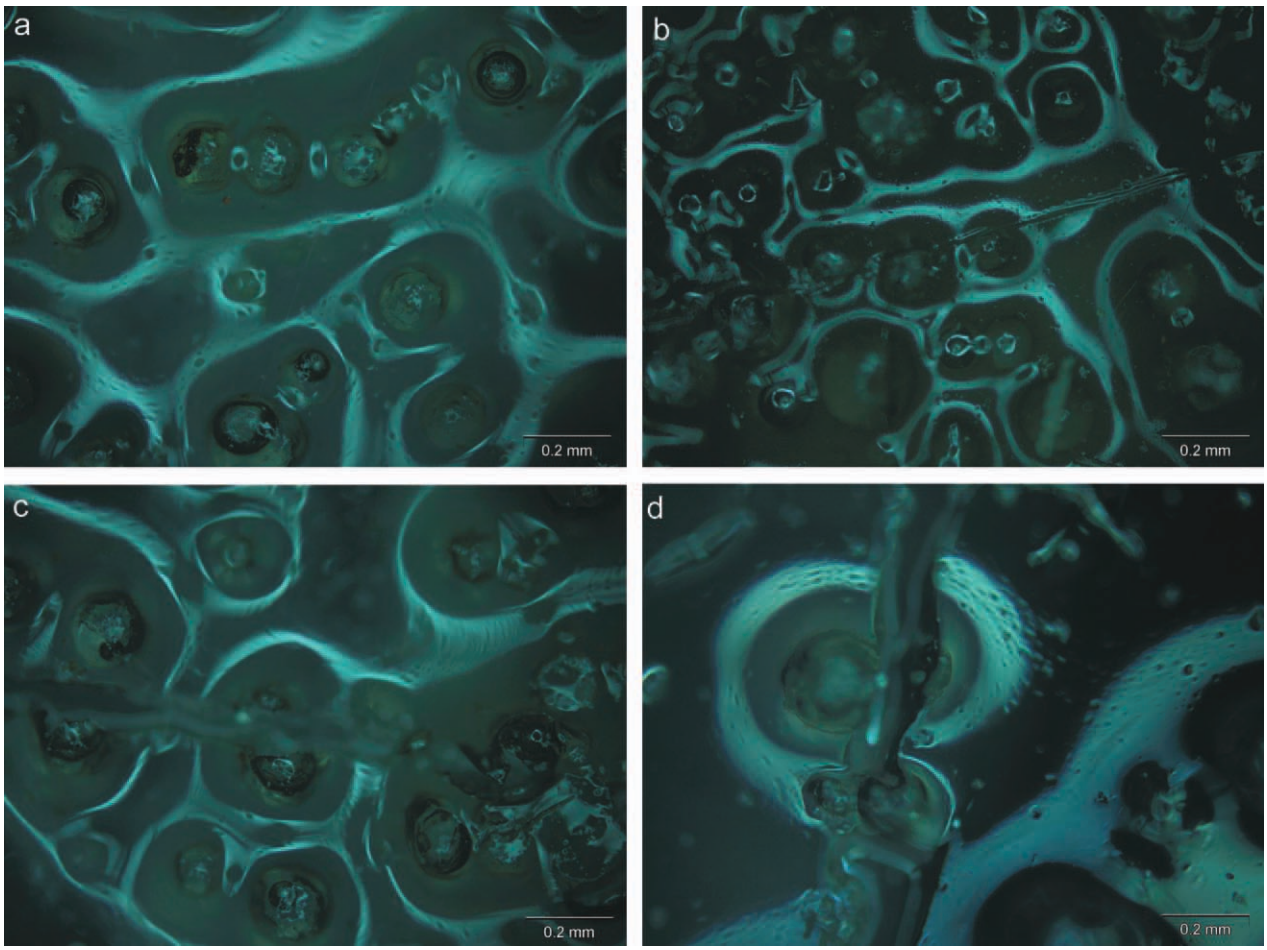

Figure 6. Self healing process of microencapsules incorporated coating on steel substrate. (a) Unscratched sample, (b) Scratched sample, (c) Scratched sample after 1 h of exposure to air, and (d) Scratched sample after 1 h of exposure to air. [Color figure can be viewed in the online issue, which is available at wileyonlinelibrary.com.]

45.32% at 873 K. The degradation temperature is lower than that of pure silicone resin, but the weight loss of this IPN is slightly higher than that of silicone resin. This indicates that the presence of entangled acrylic molecules in the IPN is limited. In the DSC analysis, an endothermic peak is observed between 448 K and 498 K accompanied by energy absorption of 9.391 J/g. This is due to the further penetration of unreacted acrylic monomer in the IPN to form a strong IPN. In the latter stage, at 573.67 K, an exothermic reaction occurs with the liberation of 18.12 J/g energy. This shows that the breaking of the silicone–acrylic linkages take place with the liberation of energy. Thus, this analysis shows that the formation of IPN is complete and only one exothermic reaction occurs during the disintegration of the IPN.

Self Healing Effect

Figure 6(a–d) shows the healing efficiency of microcapsules in IPN. It is seen from Figure 6(a) that the microcapsules are dispersed in the IPN. Figure 6(b) indicates a scratch of nearly 20 μm width is created on the surface. It is observed that the scratch is passing through some of the capsules in the composite coating. From Figure 6(c) it is observed that 1 h after the scratch is formed, the core polymer has started to flow through the scratch area. It is clearly seen from Figure 6(d) that the core polymer completely comes out of the shell and heals the entire scratched area and left the shell alone in that area. Thus this study confirms that the polymer from the microcapsule takes 24 h to complete the healing action.

Evaluation of the Healing Efficiency of the Microcapsules in 1PN

SVET Technique. The SVET diagram [Figure 7(a)] shows the performance of the self healing coating 1 h after the damage has occurred on the surface. It is observed from the figure that some anodic corrosive region is seen in red color. The green color denotes that there is no corrosion spot on the surface. The blue color points out the cathodic region of the reaction. Corrosion initiation occurs due to the exposure of the pure metal to the air immediately after the scratch formation. Figure 7(b) shows the surface, 24 h after exposure to air. It is observed that no corrosion spot is visible on the surface. Thus this photograph indicates that the complete healing of the scratch requires, at least 24 h. This study indicates that the core polymer from the ruptured microcapsules flows through the scratch and reacts with the catalyst to form cured film and prevents the initiation of corrosion. The time dependence of the corrosion processes at the scratch site followed by measuring the current density at the panels after 1 h and 24 h. The recorded scans over the scratch are given in Figure 7(c).The current density at the scratch area is much higher at 1 h. The scratch can be a source for the conduction of electrolyte through the metal surface, whereas the scratch surface is healing after 24 h, and so the peak position in the current density plots has shifted to a very low value. This shift is due to the formation of the protective film of the core polymer from the capsules on the defect area, which decrease activity at the scratch. SVET study is a tool to identify the self-healing efficiency of the microcapsules in the IPN. Self healing mechanism of galvanized steel has already been explained by current density changes on the surface by SVET and numerical modeling.[25]

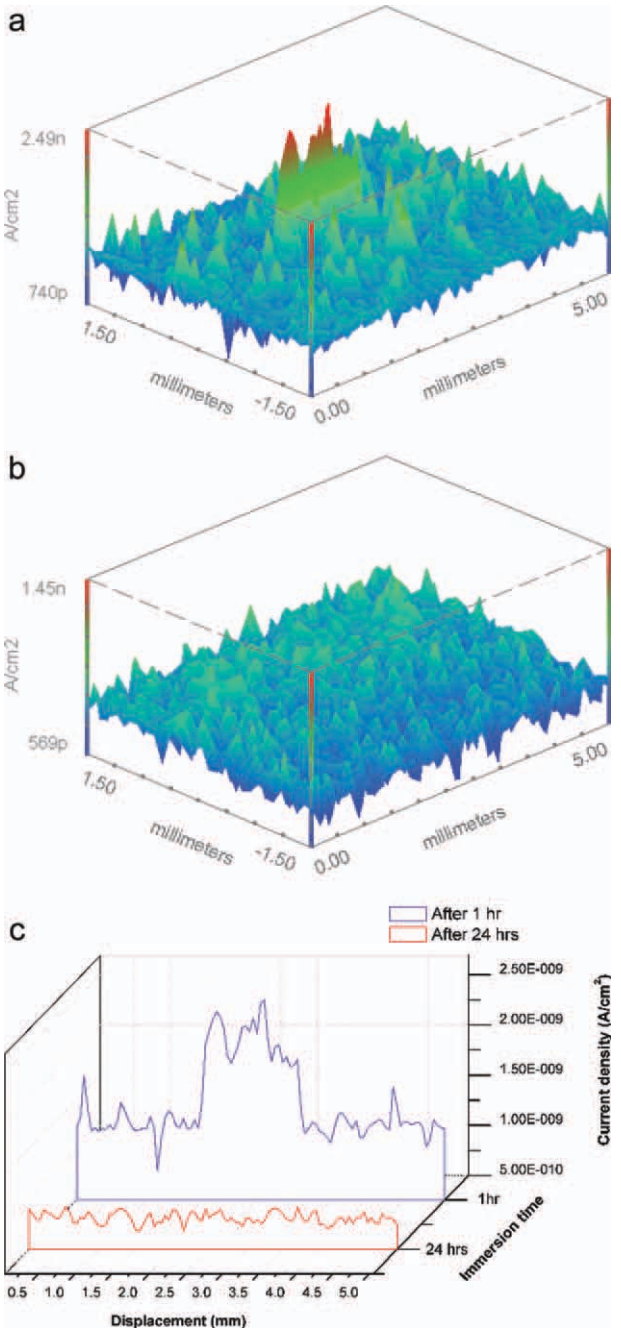

Figure 7. (a) SVET-3D representation of scratched microcapsules incorporated coating on mild steel surface after 1 h exposure to 0.05*M* NaCl solution. (b) SVET-3D representation of scratched microcapsules incorporated coating on mild steel surface after 24 h exposure to 0.05*M* NaCl solution. (c) Variation in the total current measured above the scratch in 1 h and 24 h of exposure in 0.05*M* NaCl solution. [Color figure can be viewed in the online issue, which is available at wileyonlinelibrary.com.]

2 EIS Measurement. Table II shows the resistance and capacitance values of IPN with and without microcapsule

Table II. Resistance and Capacitance Values of IPN with and Without the Microcapsules Incorporated Coating on Steel Panels in 0.05*M* NaCl Solution for1 h and 24 h Duration

Coated sample	Solution resistance (Ω/cm^2)	Double layer capacitance (F)	Charge transfer resistance (Ω/cm^2)
IPN with microcapsules (after 1 h)	3.386×10^{-2}	3.734×10^{-11}	4.277×10^{10}
IPN with microcapsules (after 24 h)	7.646×10^{-3}	3.724×10^{-11}	3.764×10^{10}
IPN without microcapsules (after 1 h)	2.193×10^{-3}	7.533×10^{-11}	3.411×10^{10}
IPN without microcapsules (after 24 h)	1.918×10^{-4}	9.608×10^{-11}	1.456×10^{10}

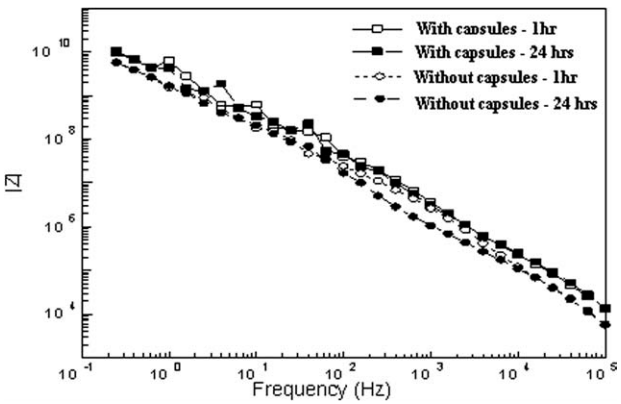

Figure 8. Bode plot of IPN and microcapsules incorporated IPN on mild steel substrate in 0.05*M* NaCl solution for 1 h and 24 h durations.

incorporated coating on steel panels, obtained from Bode plots in 0.05*M* NaCl solution for 1 h and 24 h of duration. The impedance spectra of these coated steel panels in 0.05*M* NaCl for 1 h and 24 h are shown in Figure 8. The shape of the Bode plots indicates that these coatings are capacitive in nature. The nature of the impedance spectra is slightly inclined at an angle of 45° towards the frequency axis. The impedance data shows that a slight decrease in resistance is observed after 24 h of exposure. From the table it is observed that the microcapsule incorporated coatings have higher resistance than the coatings without the capsules. These results indicate that the microcapsule incorporation in the coating has not affected the performance of the IPN on steel substrate.[26] Further, the capacitance value has not changed significantly. These values are in the order of 10^{-11} F. The capacitance values are an indication of penetration of water molecules through the coating.

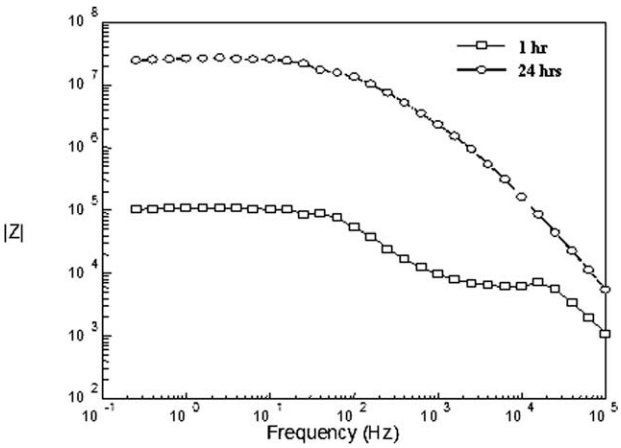

Figure 9. Bode plot of scratched microcapsules incorporated IPN in 0.05*M* NaCl solution for 1 h and 24 h exposure to air.

Figure 9 shows the Bode plots of the scratched area recorded in 0.05*M* NaCl solution after 1 h and 24 h. Corresponding resistance and capacitance values are tabulated in Table III. It is observed that the Bode plots are bending towards the "X" axis with increase of duration of immersion after 24 h. The curve starts to act as a capacitive plot after 24 h of duration, suggesting that the resistance of the coating is higher due to the healing effect of the core polymer present in the capsules. The resistance observed by the coating system always depends on the extent of penetration of the electrolyte to the substrate through the coating.[27,28] Pore resistance is the measure of the degradation of the coating. From Table III it can be observed that the resistance exerted by the coated panels after 1 h duration is 9.6×10^4 Ω/cm^2; it increases to 2.441×10^7 Ω/cm^2 after 24 h. This shows that the core polymer flow from the capsules completely fill the scratch and increase the resistance on the surface. This is further supported by the capacitance values (Table III). It can be observed that the capacitance values decreased from 2.53×10^{-8} F to 7.729×10^{-11} F after 24 h. The decrease in capacitance value suggests that the scratch is completely healed after 24 h by the core polymer and penetration of water molecule through it to reach the steel substrate is prevented. This study also clearly indicates that the healing efficiency depends on duration by which the healing agent completely fills the scratch on the surface.

CONCLUSION

Interpenetrating polymer network, prepared using silicone polymer and acrylic monomer, was characterized by FTIR and TGA/DSC analysis. Epoxy filled microencapsules were prepared and

Table III. Resistance and Capacitance Values of IPN with the Microcapsules Incorporated Coating on Steel Panels in 0.05*M* NaCl Solution with Scratch for 1 h and 24 h Duration

Scratched sample	Solution resistance (Ω/cm^2)	Double layer capacitance (F/cm^2)	Charge transfer resistance (Ω/cm^2)
A 1	8.491×10^3	2.53×10^{-8}	9.600×10^4
A 24	5.904×10^{-3}	7.729×10^{-11}	2.441×10^7

incorporated in the IPN. The morphology and self healing efficiency of these coatings were determined by microscopic methods. The self healing efficiency was evaluated by SVET. No anodic current density was observed after 24 h of duration, which is the indication of complete curing of the polymer through the crack. The EIS study confirmed that complete healing of the scratch take place within 24 h. The resistance exerted by the coating after 1 h in 0.05*M* NaCl is 9.64×10^4 Ω/cm^2, whereas resistance of the same system is 2.441×10^7 Ω/cm^2 after 24 h. It can be concluded that the SVET and EIS techniques can be used as tools for evaluating the efficiency of self-healing coatings on mild steel substrate.

REFERENCES

1. Swapan Kumar Ghosh. Functional Coatings; Weinheim: Wiley-VCH Verlag Gmbh &Co. K GaA, **2006.**
2. Kessler, M. R.; Scott, N. P. *White's Compos: Part A* **2003,** *34*, 743.
3. Dong Yang Wu, Sam Meure, Davide Solomon. *Prog. Polym. Sci.* **2008,** *33*, 478.
4. Ding Shu Xiao, Yan Chao Yuon, Min Zhi Rong, Ming Qiu Zhang. *Polymer* **2009,** *50*, 2967.
5. Staples, M. L. *Mater. Perform.* **1989,** *28*, 33.
6. Kamalan Kirubaharan, A. M.; Palraj, S.; Selvaraj, M.; Rajagopal, G. J. *Appl. Polym. Sci.* **2011,** *119*, 2339.
7. Shailesh, K. D.; Palraj, S.; Maruthan, K.; Selvaraj, M. *Prog. Org. Coat.* **2007,** *59*, 21.
8. Rohewerder, M.; Michalic, A. *Electrochem. Acta* **2007,** *53*, 1300.
9. Ocampo, C.; Armetin, E. *Prog. Org. Coat.* **2005,** *53*, 217.
10. Gok, A.; Omastova, M.; Gulyavuz, A. *Synth. Met.* **2007,** *157*, 23.
11. Lu, M.; Li, X.; Hu-Lin, L. *Mater. Sci. Eng.* **2004,** *334*, 291.
12. San, B.; Talu, M.; Yildrum, F.; Balct, E. K. *Appl. Surf. Sci.* **2003,** *205*, 27.
13. Zielecka, M.; Bujuowska, E. *Prog. Org. Coat.* **2006,** *55*, 160.
14. Kamalan Kurubakaran, A. M.; Palraj, S.; Selvaraj, M.; Rajagopal, G. J. *Appl. Polym. Sci.* **2011,** *119*, 2339.
15. Khramov, A. N.; Voevodin, N. N.; Balbyshev, V. N.; Donley, M. S. *Thin Solid Films* **2004,** *447*, 549.
16. Dmitry, G.; Shchukin, M. Z.; Helmuth, M. J. *Mater. Chem.* **2006,** *16*, 4561.
17. Dmitry, G. S.; Dmitry, O. G.; Helmuth, M. *Soft Matter* **2010,** *6*, 720.
18. Mansfeld, F. J. *Appl. Electrochem.* **1995,** *25*, 187.
19. Suryanarayanaa, C.; Chowdoji Raob, K.; Dhirendra Kumar. *Prog. Org. Coat.* **2008,** *63*, 72.
20. Samadzadeh, M.; Hatami Boura, S.; Peikari, M.; Kasiriha, S. M.; AShrafi, A. *Prog. Org. Coat.* **2010,** *68*, 159.
21. Luz Sanchez; Paula Sanchez; Antonio de Lucas; Manuel Carmona; Juan, F. R. *Colloid Polym. Sci.* **2007,** *283*, 1377.
22. Suna, G.; Zhang, Z. *Int. J. Pharm.* **2002,** *242*, 307.
23. Tiwari, A.; Hahira, L. H. *Polym. Degrad. Stab.* **2009,** *94*, 1754.
24. Mu, J. F.; Liu, Y.; Zheng, S. *Polymer* **2007,** *48*, 1176.
25. Florian The'bault, Bruno Vuillemin, Roland Oltra, Kevin Ogle, Christian Allely. *Electrochimica Acta* **2008,** *53*, 5226.
26. Taryba, M.; Lamaka, S. V.; Snihirova, D.; Ferreira, M. G. S.; Montemor, M. F.; Wijting, W. K.; Toews, S.; Grundmeier, G. *Electrochimica Acta* **2011,** *56*, 4475.
27. Suay, J. J.; Bodriguez, M. T.; Ruzzalp, K. A.; Capiro, J. J.; Saura, J. J. *Prog. Org. Coat.* **2003,** *46*, 121.
28. Yin, K. M.; Lu, L. L. *J. Coat. Technol.* **2003,** *75*, 65.